Annual sea level amphidromes in the South China Sea revealed by merged altimeter data

Caiyun Zhang,[1] Bin Wang,[2] and Ge Chen[1]

Received 3 April 2006; revised 8 June 2006; accepted 13 June 2006; published 20 July 2006.

[1] Annual phase-amplitude characteristics of sea level anomaly (SLA) in the South China Sea (SCS) are investigated by a merged SLA data set derived from simultaneous measurements of Envisat, Geosat-Follow-on (GFO), Jason-1, and TOPEX/Poseidon (T/P) from January 2004 to December 2005. Four annual amphidromes instead of two are revealed and their locations, surrounding the Vietnam eddy, distinguish two distinctive regimes of annual variations in the SCS, a basin scale monsoon regime and a local Vietnam eddy regime. Their existence suggests that the annual amphidrome is not only a common feature on global scale, but also a phenomenon in regional seas. However, the locations of these amphidromes in the SCS vary considerably from year to year, in contrast to the annual amphidomes found in the tropical ocean basins, which are much more stable. **Citation:** Zhang, C., B. Wang, and G. Chen (2006), Annual sea level amphidromes in the South China Sea revealed by merged altimeter data, *Geophys. Res. Lett.*, *33*, L14606, doi:10.1029/2006GL026493.

1. Introduction

[2] As a primary mode of sea level (SL) variability, the annual SL variation in the South China Sea (SCS) has been studied extensively during the past decade, in particular, with the advent of data from satellite altimetry [*Shaw et al.*, 1999; *Ho et al.*, 2000; *Morimoto et al.*, 2000; *Hwang and Chen*, 2000; *Q. Liu et al.*, 2001; *Z. Liu et al.*, 2001]. In fact, the annual SL variation can be considered as an annual tide in terms of its property and its corresponding amphidromes can be identified in the SCS. As a scientific term in describing the tidal system, an "amphidrome" normally refers to an oceanic point where there is zero tidal amplitude due to canceling of tidal waves. Recent studies by *Chen and Quartly* [2005] illustrated that an amphidrome is not a tide-only phenomenon in the ocean, but a common feature existing in the global annual SL and sea surface temperature (SST) variations. These interesting findings lead to the speculation that annual amphidromic system of this kind might exist as well in regional seas where annual variations are very energetic. But this requires much higher quality and resolution of satellite data than those used for global scale study. This letter focuses on identification of annual SL amphidromic system in the SCS by analyzing the phase-amplitude characteristics of SLA derived from a newly merged product of simultaneous measurements of four altimeters. Previous studies indicate that the phase-amplitude features of key parameters in the coupled air-sea system can reveal new aspects of climate variation [e.g., *Wang et al.*, 2000; *Chen and Lin*, 2005]. The result serves as a useful contribution to our knowledge and understanding of the annual variation in SLA in the SCS.

2. Satellite Data

[3] Since February 2004, a merged SLA product from simultaneous SL measurements of four altimeters, Envisat, GFO, Jason-1, and T/P, has been released by Archiving, Validation and Interpretation of Satellite Oceanographic data (AVISO). The merged SLA data have, for the first time, two years' record before the termination of T/P in January 2006. The mapping skills for merging multi-altimeter missions have been detailed by *Le Traon et al.* [2003], and *Le Traon and Dibarboure* [2004]. This product has the superior quality and best mapping capability for mesoscale SL variation according to *Le Traon and Dibarboure* [1999], and is further illustrated by its comparison with the products from single-altimeter missions [*Zhang and Chen*, 2006]. One hundred and four weekly maps spanning January 2004 through December 2005 have been compiled in this study. Note that the merged data from four missions were released since February 2004, therefore, for the integrity of data in 2004, the merged data from the first three missions also have been compiled in this study. All the original data have had the standard altimetry corrections applied, including a full tidal model. Results distributed over marginal seas with depths less than 100m are not considered due to the large contamination of altimeter-derived SLA over shallow water. We expect that the two-year record of SLA is adequate for examining annual variation during this period.

3. Results

3.1. Fractional Variances of the Annual and Semiannual Harmonics

[4] Previous studies indicate that the annual cycle (AC) and semiannual cycle (SC) dominate SL variations in the SCS [*Hwang and Chen*, 2000]. Before going to phase-amplitude analysis, understanding of the relative importance of the AC and SC is very helpful. This can be quantified by estimating the ratio of their amplitudes for the SCS, as illustrated in Figures 1a and 1d. The area-averaged ratios in the SCS are roughly estimated to be 2.0 and 2.6 in 2004 and 2005, respectively, suggesting that AC is more prominent than SC in magnitude and the year-to-year variation is also significant. The relationship between the ratio plots and the amphidromic issue will be discussed in the following sections.

[1] Ocean Remote Sensing Institute, Ocean University of China, Qingdao, China.
[2] International Pacific Research Center, University of Hawaii at Manoa, Honolulu, Hawaii, USA.

0094-8276/06/2006GL026493$05.00

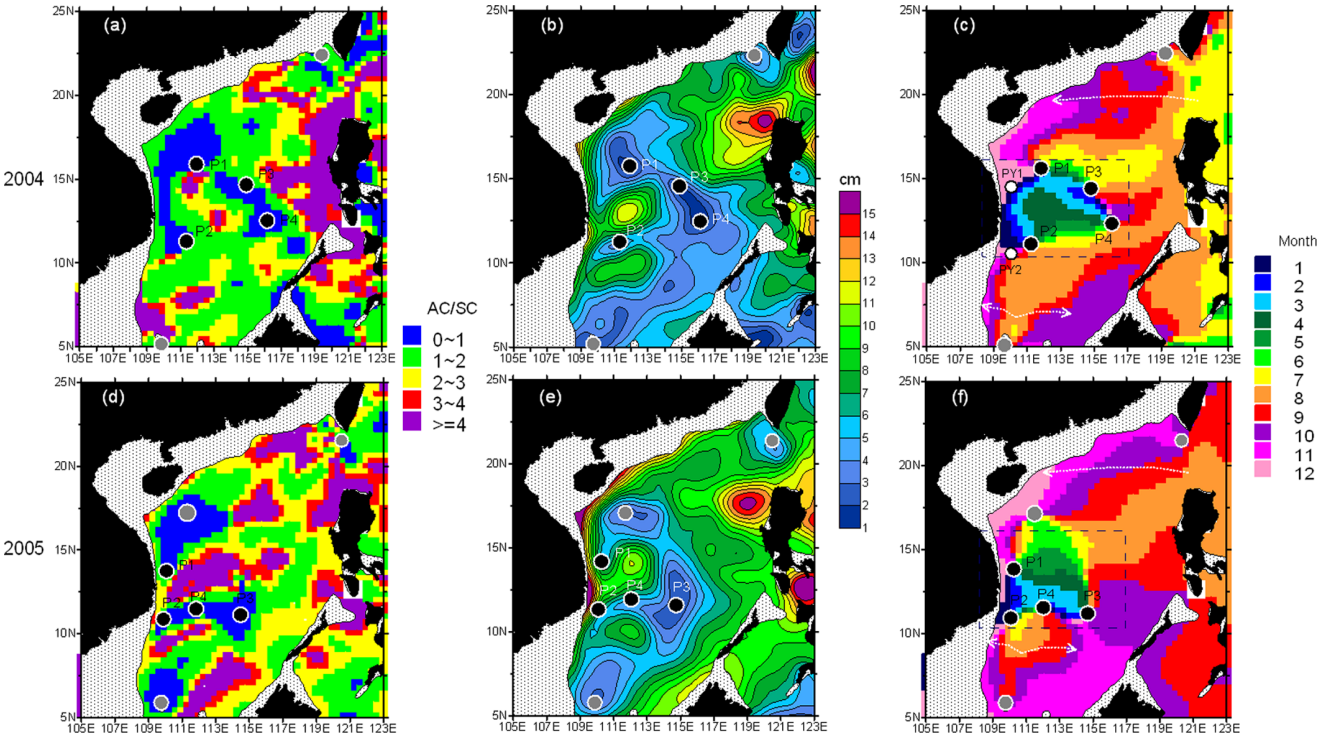

Figure 1. (a) Geographical distribution of the ratio of AC vs SC amplitude of SLA, (b) the amplitude map of the annual sea level (SL) variation, and (c) map of calendar month during which the annual SL reaches its peak in 2004. (d–f) Same as Figures 1a–1c but for 2005. Four annual amphidromes are highlighted by the black solid dots, and two annual amphidromes identified by *Yanagi et al.* [1997] are indicated in Figure 1c by white solid dots. The gray solid dots are the ill-defined annual amphidromes in 2004 and 2005. The white dashed arrow curves in Figures 1c and 1f depict the phase propagation, and the reversal phase structure in the western center of the SCS is in blue dashed rectangle.

3.2. Annual Amplitude-Phase Diagram

[5] The annual amplitudes of SLA in 2004 and 2005 are displayed in Figures 1b and 1e, respectively. Two maps in 2004 and 2005 show eddy-like structures with maxima off northwest of the Luzon Island (red) and minima in the central SCS (blue). Moreover, a tongue-like structure with high amplitude extends from the east of Vietnam to 113°E (yellow in 2004 and green in 2005), and a southwest-northeast oriented broad band with small annual variation is located in the southern SCS, which connects with a southeast-northwest orientated band of small amplitude from the central to northwestern SCS (blue). The small-amplitude AC regions bear some similarity with the pattern of the low ratio regions in Figures 1a and 1d, but they are not identical, because the ratio is not only determined by the amplitude AC, but also the amplitude of SC, thus it reflects some information of the SC component. Note that the large amplitude variation found off northwest Luzon and off Vietnam coast around 12°N are caused by seasonal upwelling due to monsoon-induced off-shore Ekman transports. Annual SLA phase patterns in 2004 and 2005 are displayed in Figures 1c and 1f. An overall impression is that most regions reach their annual maximum in July–December, but a distinct reversal of the phase pattern is seen over the western central SCS where it peaks in January–June. Three distinguished regional phase propagation regimes can be identified and highlighted by the white dashed arrow curves and blue dashed rectangle in Figures 1c and 1f, which will be examined in the next two paragraphs.

[6] In the northern SCS (north of 17°N), the annual phase propagates westward with a speed of approximately 3 degrees/month. This consistent phase propagation is closely connected with a forced annual Rossby wave identified by *Yang and Liu* [2003]. In the southern SCS, the sea level reaches a maximum in July and August around 110°E followed by progressively later occurrence toward both the east and west. A detailed comparison between 2004 and 2005 illustrates about one month delay for 2005 to reach its high SL than 2004 in the northern and southern SCS.

[7] Compared with the northern and southern SCS, the annual phase propagation in the central SCS (from 10°N to 17°N) is much more complex. Its annual maximum occurs in January–June over the western central SCS, and in July–December over the eastern central SCS. Based on longitude-time plots of SL data derived from T/P and Levitus, *Z. Liu et al.* [2001] suggested that SLA exhibits a westward propagation north of 18°N, while eastward propagation south of 18°N. The detailed SLA propagation patterns indicate the annual SLA propagation is not simply eastward south of 18°N, instead, it exhibits a basin-scale rotary propagation with co-phase lines irradiating from certain points. These interesting findings imply that annual SL amphidromic system exists in the central SCS.

3.3. Annual Sea Level Amphidromes

[8] An "amphidrome" is characterized by its undetermined phase and almost zero amplitude. In the large portion

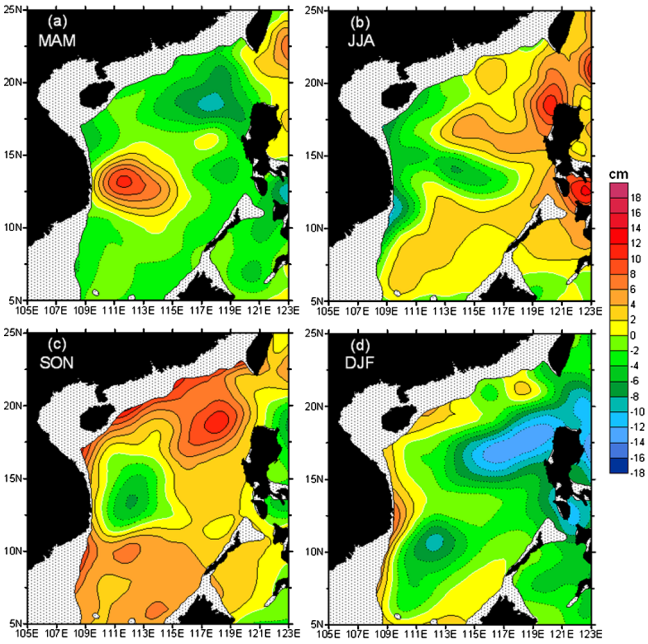

Figure 2. Seasonal distribution of SLA in the SCS. (a) Spring (March–May), (b) summer (June–August), (c) autumn (September–November), and (d) winter (December–February). The dotted black, thin black, and thick white curves denote negative, positive, and zero contours, respectively.

of the SCS, clear rotary systems circling four nodal points, P1, P2, P3, and P4 constitute a salient feature of the annual SLA phase propagation in Figures 1c and 1f. The P1 and P2, located at (111.9°E, 15.6°N) and (111.2°E, 11.1°N), (110.3°E, 13.8°N) and (110.1°E, 10.9°N), in 2004 and 2005, respectively, are close to the two locations that are briefly reported by *Yanagi et al.* [1997] using T/P-derived altimetry data. The locations found by them are displayed by the white solid dots in Figure 1c. The annual SLA phase detected from the merged SLA data does provide direct evidence of the existence of these two annual amphidromes in the SCS. Moreover, the annual phase structure around P1 and P2 presents a reversal pattern with cyclonic rotation around P1 and anticyclonic around P2.

[9] Besides P1 and P2, another pair of amphidromes, P3 and P4, located at (114.8°E, 14.4°N) and (116.0°E, 12.3°N), and (114.7°E, 11.2°N) and (112.0°E, 11.5°N), for 2004 and 2005, respectively, are firstly detected in the SCS owing to the unprecedented quality and resolution of altimetry data from the four missions. Annual sea level rotates anticyclonically around P3 with an uneven phase rate, while P4, sharing the co-phase lines with P3 from August to next March in 2004 and January–March in 2005, has shown a reversal pattern of phase propagation around it. The four well-separated nodal points, P1, P2, P3, and P4, sharing co-phase lines in January–April over the central part of SCS, are closely connected with each other. It seems that the annual phase propagation is largely controlled by primary amphidromes, P1 and P2, over the entire SCS, and further modulated locally by secondary amphidromes, P3 and P4, over the central part of SCS.

[10] As a further examination of these annual amphidromes existing in the SCS, their geographical locations are projected over the related annual amplitude plots in Figures 1b and 1e, as well as the ratio patterns in Figures 1a and 1d. These four nodal points are indeed located in the regions where the amplitudes of AC are very small. All of them are also located in regions where SC signals are stronger than the AC. The low ratio region is a better indicator for existence of amphidrome than the absolute amplitude of AC in Figures 1b and 1e, suggesting that the amphidromes reflect additional information about the SC component. Furthermore, a combining observation of phase and amplitude diagrams seems to show some other unformed amphidromes highlighted by the gray solid dots in Figure 1, where low amplitudes and ill-defined rotating patterns are discernible. These well-defined and ill-defined annual amphidromes form a fundamental feature of annual SL variation in the SCS. Note that the comparison of 2004, 2005, as well as *Yanagi et al.* [1997] shows that the locations of these amphidromes in the SCS vary considerably from year to year. This is another interesting finding, in contrast to the previous study of the tropical oceans, annual SL amphidromes are much more stable with small changes of locations within 1°–2° [*Chen and Quartly*, 2005].

4. Discussion

[11] Different from a tidal amphidrome, which has a mature Kelvin wave theory to explain it, the annual SL amphidrome is just a new issue raised by *Chen and Quartly* [2005]. The dynamics behind them is associated with meteorological forcings. All previous studies illustrate that the annual SL variation in the SCS is forced mainly by seasonal variations of monsoon. Before we discuss the formation of these annual amphidromes in the SCS, the seasonal distribution of SLA during the past two years in the SCS can be informative, as illustrated in Figure 2.

[12] The winter and summer patterns are nearly mirror image to each other. During winter the northeast monsoon induces upwelling northwest of Luzon and westward Ekman transport tends to pile up water in the west; thermocline adjusts accordingly and yields a deeper (shallower) thermocline in the west (east). The effects of summer southwest monsoon are just opposite to that of the northeast winter monsoon. The basin wide annual variation in SLA is a response to the monsoon forcing. The spring and autumn SLA distributions also share an opposite pattern with a notable SLA eddy being observed to the east of Vietnam, where the annual variation of SLA distinguished from all other regions of the SCS: It is positive in spring while negative in autumn and has negative polarity compared with rest of the SCS basin (Figures 2a and 2c). In addition, in that region, annual variations are 90° of out of phase with the rest of the SCS region and around it annual amphidromes are identified.

[13] Therefore, explanation of the annual variation of this Vietnam eddy may hold a key to interpretation of the existence of the four annual amphidromes. In theory, an eddy with negative (positive) SLA is produced by cyclonic (anticyclonic) wind stress curl that can produce divergence (convergence) in the surface water and upwelling (downwelling). According to *Shaw et al.* [1999], the SL variation in

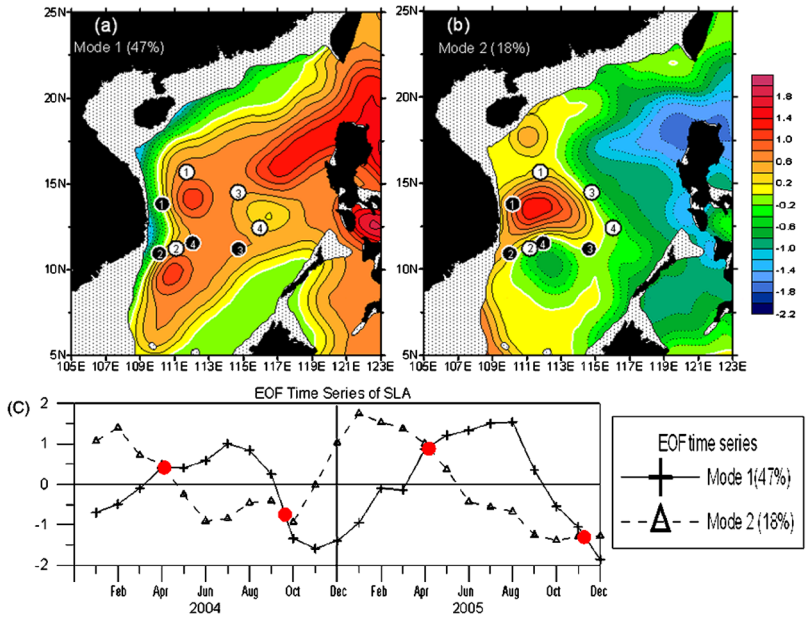

Figure 3. (a–c) The first two modes of EOF analysis of SLA. The dotted black, thin black, and thick white curves in Figures 3a and 3b denote negative, positive, and zero contours, respectively. The thin black and dashed black curves in Figure 3c refer to the first and second modes of EOF time series and the thin black horizontal line denotes zero. White and black dots in Figures 3a and 3b are the locations of four annual amphidromes in 2004 and 2005, and red dots in Figure 3c highlight the intersection of the mode 1 and mode 2.

the SCS consists of two leading modes, which correspond well to the first two modes of the wind stress curl and both of them have an obvious annual cycle. Their results inspire us to explain the formation of these annual amphidromes with the use of EOF analysis. The EOF results are presented in Figure 3. Mode 1 and mode 2 together can explain 65% of the variance and both of them have a clear annual period. The first mode is consistent with the set-up and set-down of water in the western basin in winter and summer induced by seasonal wind stress over the SCS (Figures 3a, 2b, and 2d). The EOF time series of the first mode displays that it reaches its maximum and minimum in July and November in 2004, and in August and December in 2005, which confirms the delay SL season occurred in 2005 (Figures 3c, 1c, and 1f). The second mode mainly contributes to the Vietnam eddy and Luzon Strait and note that they share an opposite polarity (Figure 3b). Mode 2 displays its extremes in February and October for 2004, while in January and October for 2005 (Figure 3c). Therefore, the whole annual variation of SL in the SCS is mainly controlled by the first mode and slightly modulated by the second mode. Since the two modes have an obvious annual period, when their effects are of equal amplitude and exactly out of phase, there is no net seasonal signal. This will produce the well-determined nodal points over this region. Another interesting finding of the EOF time series of mode 1 and mode 2 in Figure 3c is that two modes intercross in April and around October (November) in 2004 (2005), which is just associated with the annual SL seasons defined in Figures 1c and 1f over the Vietnam eddy region. P1 and P2, P3 and P4, are located around the zero contour curves of mode 1 and mode 2, respectively, which suggests that the locations of P1 and P2, P3 and P4, are mainly modulated by mode 1 and mode2, respectively. Further, all of them are located in the western central SCS, surrounding the spring maximum and fall minimum of SLA (Figures 2a and 2c), as well as the variability center of EOF2 mode (Figure 3b), which implies that their existence results from the unique seasonal variation of the SLA over the Vietnam eddy region. Because the behavior of the eddy is subject to interannual variations in the forcing field, the locations of amphidomes vary accordingly. Therefore the locations of these amphidromes are unstable and the different locations indicated by *Yanagi et al.* [1997] and our results in 2004 and 2005 can be explained.

5. Summary

[14] Annual phase-amplitude diagrams of SLA derived from the merged dataset of four altimeters convey rich information about the annual SL variations in the SCS. First, it provides more detailed phase propagations in the SCS, which is more than what time-longitude plots can reveal. Second, four instead of two well-defined annual SL amphidromes are identified, which suggests that annual SL variation (in time) is characterized by a basin-wide rotary propagation of the annual phase (in space). Third, the year-to-year variation of these annual amphidromes' locations is very significant in the SCS due to the large interannual forcing field.

[15] The existence of these annual amphidromes is intriguing and the identification of their locations are important, because in theory, they are free of interference of energetic seasonal signals; therefore they are ideal locations for deployment of gauges and buoys for effective and efficient observations of other SL variation modes. However, it is a pity that we have only two-year data in SLA records, which make the statistical separation of the clima-

tological feature and interannual variability very difficult. We are currently examining model simulated SL field to address the question, and the reliability of the derived results in this study can be tested with accumulation of higher resolution altimetry data and oceanic models in our future studies.

[16] **Acknowledgments.** This study is cosponsored by the National Basic Research Program of China (project 2005CB422308) and the Natural Science Foundation of China (project 40545018). Satellite data are provided by AVISO. Bin Wang acknowledges support of NOAA/CLIVAR project.

References

Chen, G., and H. Lin (2005), Impact of El Niño/La Niña on the seasonality of oceanic water vapor: A proposed scheme for determining the ITCZ, *Mon. Weather Rev.*, *133*, 2940–2946.

Chen, G., and G. D. Quartly (2005), Annual amphidromes: A common feature in the ocean?, *IEEE Geosci. Remote Sens. Lett.*, *2*, 423–427.

Ho, C. R., Q. Zheng, Y. S. Soong, N. J. Kuo, and J. H. Hu (2000), Seasonal variability of sea surface height in the South China Sea observed with TOPEX/Poseidon altimeter data, *J. Geophys. Res.*, *105*(C6), 13,981–13,990.

Hwang, C., and S. A. Chen (2000), Fourier and wavelet analyses of TOPEX/Poseidon-derived sea level anomaly over the South China Sea: A contribution to the South China Sea Monsoon Experiment, *J. Geophys. Res.*, *105*(C12), 28,785–28,804.

Le Traon, P. Y., and G. Dibarboure (1999), Mesoscale mapping capabilities of multi-satellite altimeter missions, *J. Atmos. Oceanic Technol.*, *16*, 1208–1223.

Le Traon, P. Y., and G. Dibarboure (2004), An illustration of the contribution of the TOPEX/Poseidon–Jason-1 tandem mission to mesoscale variability studies, *Mar. Geod.*, *27*, 3–13.

Le Traon, P. Y., Y. Faugère, F. Hernandez, J. Dorandeu, F. Mertz, and M. Ablain (2003), Can we merge GEOSAT Follow-On with TOPEX/Poseidon and ERS-2 for an improved description of the ocean circulation?, *J. Atmos. Oceanic Technol.*, *20*, 889–895.

Liu, Q., Y. Jia, X. Wang, and H. Yang (2001), On the annual cycle characteristics of the sea surface height in the South China Sea, *Adv. Atmos. Sci.*, *18*, 613–622.

Liu, Z., H. Yang, and Q. Liu (2001), Regional dynamics of seasonal variability in the South China Sea, *J. Phys. Oceanogr.*, *314*, 272–284.

Morimoto, A., K. Yoshimoto, and T. Yanagi (2000), Characteristics of sea surface circulation and eddy field in the South China Sea revealed by satellite altimetric data, *J. Oceanogr.*, *56*, 331–344.

Shaw, P.-T., S. Y. Chao, and L. L. Fu (1999), Sea surface height variation in the South China Sea from satellite altimetry, *Oceanol. Acta*, *22*, 1–17.

Wang, B., R. Wu, and R. Lukas (2000), Annual adjustment of the thermocline in the tropical Pacific Ocean, *J. Clim.*, *13*, 596–616.

Yanagi, T., T. Takao, and A. Morimoto (1997), Co-tidal and co-range charts in the South China Sea derived from satellite altimetry data, *Lar Mer*, *35*, 85–93.

Yang, H., and Q. Liu (2003), Forced Rossby wave in the northern South China Sea, *Deep Sea Res., Part I*, *50*, 917–926.

Zhang, C., and G. Chen (2006), A first comparison of simultaneous sea level measurements from Envisat, GFO, Jason-1, and TOPEX/Poseidon, *Sensors*, *6*, 235–248.

C. Zhang and G. Chen, Ocean Remote Sensing Institute, Ocean University of China, 5 Yushan Road, Qingdao 266003, China. (zhangcy@orsi.ouc.edu.cn)

B. Wang, International Pacific Research Center, University of Hawaii at Manoa, 1680 East West Road, Honolulu, HI 96822, USA.